PAIR Diffusion: A Comprehensive Multimodal Object-Level Image Editor

Supplementary Material

This appendix contains three sections organized as follows. In Sec. 6 we discuss our proposed multimodal classifier free guidance, proving Eq. (4) of the main paper and providing qualitative results for its usage. In Sec. 7, we report the implementation details of our unconditional model along with details about the baselines adopted in the paper. Lastly, in Sec. 8 we show additional qualitative results and applications of our framework. Please refer to our arXiv version[1] for high-quality images.

6. Multimodal Classifier Free Guidance

6.1. Proof

Let us represent $p(z|c)$ as the distribution we want to learn. In our case, the conditioning $c = (S, F, y)$, while z represents the input image x in latent space. A well-trained diffusion model learns to estimate $\nabla_{z_t} \log p(z_t|c)$. Using Bayes' rule and taking the logarithm, we obtain:

$$\log p(z_t|c) = \log p(c|z_t) + \log p(z_t) - \log p(c) \tag{6}$$

In our setting of multimodal conditioning, we want to control the final image using the appearance from the reference image F and the text prompt y *independently*. Multimodal inference would be particularly useful when the information in y is disjoint from (S, F), and we need to capture it in the final image. Following this assumption, we obtain:

$$\begin{aligned} \log p(c) &= \log p(S, F, y) \\ &= \log p(S, F) + \log p(y) \end{aligned} \tag{7}$$

Similarly, expanding $\log p(c|z_t)$ and using Eq. (7):

$$\begin{aligned} \log p(c|z_t) &= \log p(S, F, y|z_t) \\ &= \log p(S, F|z_t) + \log p(y|z_t) \end{aligned} \tag{8}$$

Plugging the Eq. (7)-Eq. (8) in Eq. (6), and applying Bayes' rule:

$$\begin{aligned} \log p(z_t|S, F, y) &= \log p(S, F|z_t) + \log p(y|z_t) \\ &\quad + \log p(z_t) - \log p(S, F, y) \\ &= \log p(S, F|z_t) + \log p(y|z_t) \\ &\quad + \log p(z_t) - \log p(S, F) - \log p(y) \\ &= \log p(z_t|S, F) + \log p(z_t|y) - \log p(z_t) \end{aligned} \tag{9}$$

[1] https://arxiv.org/abs/2303.17546

Taking gradient w.r.t. ∇_{z_t} we can get

$$\begin{aligned} \nabla_{z_t} \log p(z_t|S, F, y) = &\ \nabla_{z_t} \log p(z_t|S, F) \\ &+ \nabla_{z_t} \log p(z_t|y) \\ &- \nabla_{z_t} \log p(z_t) \end{aligned} \tag{10}$$

Next, we apply Bayes' rule to the first term:

$$\begin{aligned} \nabla_{z_t} \log p(z_t|S, F) = &\ \nabla_{z_t} \log p(F|S, z_t) \\ &+ \nabla_{z_t} \log p(S|z_t) \\ &+ \nabla_{z_t} \log p(z_t) \\ &- \cancelto{0}{\nabla_{z_t} \log p(S, F)} \end{aligned} \tag{11}$$

and the second term:

$$\begin{aligned} \nabla_{z_t} \log p(z_t|y) = &\ \nabla_{z_t} \log p(y|z_t) \\ &+ \nabla_{z_t} \log p(z_t) \\ &- \cancelto{0}{\nabla_{z_t} \log p(y)} \end{aligned} \tag{12}$$

Pluggin Eq. (11)-Eq. (12) in Eq. (10) we obtain:

$$\begin{aligned} \nabla_{z_t} \log p(z_t|S, F, y) = &\ \nabla_{z_t} \log p(F|S, z_t) \\ &+ \nabla_{z_t} \log p(S|z_t) \\ &+ \nabla_{z_t} \log p(y|z_t) \\ &+ \nabla_{z_t} \log p(z_t) \end{aligned} \tag{13}$$

We can use the concept of classifier-free-guidance [16] to approximate the above equation using a single model which has been trained by dropping the conditions during training and get the final sampling equation Eq. (4):

$$\begin{aligned} \tilde{\epsilon_\theta}(z_t, S, F, y) = &\ \epsilon_\theta(z_t, \phi, \phi, \phi) \\ &+ s_S \cdot (\epsilon_\theta(z_t, S, \phi, \phi)) - \epsilon_\theta(z_t, \phi, \phi, \phi)) \\ &+ s_F \cdot (\epsilon_\theta(z_t, S, F, \phi) - \epsilon_\theta(z_t, S, \phi, \phi)) \\ &+ s_y \cdot (\epsilon_\theta(z_t, \phi, \phi, y) - \epsilon_\theta(z_t, \phi, \phi, \phi)) \end{aligned} \tag{14}$$

6.2. Ablation on CFG control parameters

The multimodal classifier free guidance has three control parameters namely s_S, s_F, s_y. In practice, the values s_S, s_F, s_y can be understood as the guidance strengths to

control how the final image is affected by the structure, reference image, and the given text prompt. When using it to edit real-world images it is crucial to understand how they change the output image when varied together. In this section, we study the effect of (a) varying structure guidance s_S and reference image guidance s_F (b) varying text prompt guidance s_y and reference image guidance s_F.

Structure (s_s) and Appearance (s_F). We explain the importance of parameters by choosing a reference image that is completely different from the underlying structure in the input image. The results are shown in Fig. 7. We can observe that as we increase s_F the model forcefully imposes the reference image appearance on the object being edited and the object starts losing its structural integrity. We can get back the structural integrity when increasing s_S as well. Notice, in the second row, when $s_F = 4$ and $s_S = 2$ we cannot see any parts of the car such as the wheel, headlight, windshield, *etc*. When we start increasing s_S the subpart of the car starts appearing the edited region starts looking more like a car. However, when we increase s_F too much as in the last row, even after increasing s_S does not help much. In general, it is good practice to keep $s_S > s_F$ when editing real images. Further, we can adjust s_F how closely we want the edited output to follow the reference appearance.

Text Prompt (s_y) and Appearance (s_F). We analyze the effect of two crucial guidance parameters that help us in controlling and editing images in a multimodal manner. The results are shown in Fig. 8. We can see that it is crucial to keep $s_y > s_F$ to see the effects of the text prompt on the output image. Further, we can see that the model is more sensitive to the s_F parameter compared to s_y. Even if we increase s_F slightly we can see diminishing effects of the prompt on the edited image. In general, when editing images in a multimodal manner it is a good practice to keep $s_y > s_F$, s_F should have a low value in an absolute sense. Keeping these constraints we can vary the parameters to adjust the final output as needed.

7. Implementation Details

7.1. PAIR Diffusion

Unconditional Diffusion Model. In this section, we provide additional details for implementing PAIR Diffusion framework on unconditional diffusion models. We used LDM [38] as our base architecture and trained on LSUN Church, Bedroom, and CelebA-HQ datasets. To extract the structure information, we apply SeMask-L [19] with Mask2former [7] trained on ADE20K [61], and compute the segmentation mask for LSUN Church and Bedroom datasets [56]. In CelebA-HQ, ground truth segmentation masks are available. Given the simplicity of the architecture and the training datasets, we found that simply using the features extracted by the VGG network (G^{Vl_1}, see Sec. 3) to be sufficient in this case to achieve various editing capabilities. To condition the model on this information, we simply concatenate G^{Vl_1} to the noisy latent z_t along the channels dimension. We increase the number of channels of the first convolutional layer of the UNet from C_{in} to $C_{in} + C + 1$, with C the number of channels in G^{Vl_1}, and keep the rest of the architecture as in [38]. For all three datasets namely, LSUN Church, Bedroom, and CelebA-HQ we start with the pretrained weights provided by LDM [38] and finetune with the same hyperparameters mentioned in the paper [38]. The number of steps, learning rate, and batch size are reported in Tab. 4. We train our models using A100 GPUs. During training, we randomly dropped structure and appearance conditioning with a probability of 10%. At inference time, we adapt Eq. (4) for sampling from the model by setting $s_y = 0$ and use classifier-free guidance style sampling using the DDIM algorithm [45] with 250 steps.

Foundational Diffusion Model. We use Stable Diffusion (SD) [38] as our base architecture and ControlNet [59] to efficiently condition SD. We use COCO [4] dataset for the experiments, which contains panoptic segmentation masks and image captions. In vanilla ControlNet, the conditioning signal is passed through a zero convolution network and added to the input noise after being passed through the first encoder block of the control module. Similarly, we utilize G^{Vl_1} in the same fashion, employing it as input to the control module as in the standard ControlNet approach. Furthermore, we modulate the features in the first encoder block of the control module using G^{Dl_2} and in the second encoder block using G^{Dl_3} by adding them to the respective features after cross-attention blocks. Before adding G^{Dl_2}, G^{Dl_3} we pass them through two linear layers to match the dimension of the features of the network. We train the network as described in ControlNet [59], training the control module and the linear layers while keeping all the other parameters frozen. We perform a grid search to identify the layers of the VGG and DINOv2 that achieve the best results. We found $l_1 = 1, l_2 = 6, l_3 = 18$ to yield the best results. During training, we randomly dropped structure, appearance, and text conditioning with a probability of 10%. Our model is trained across 4 A100 machines with 8 GPUs requiring 3 days to train the model. The number of steps, learning rate, and batch size are reported in Tab. 4. At inference time, we apply Eq. (4) for sampling and use classifier-free guidance style sampling using the DDIM algorithm [45] with 20 steps.

7.2. Baselines

Quantitative Experiments. We provide additional details about implementation and evaluation procedures for the results shown in Sec. 4.2 of the main paper. We evaluate the models on the task of in-domain appearance manipulation. We first describe the data-collection procedure. We use 5000 images from the validation set of LSUN Bedroom,

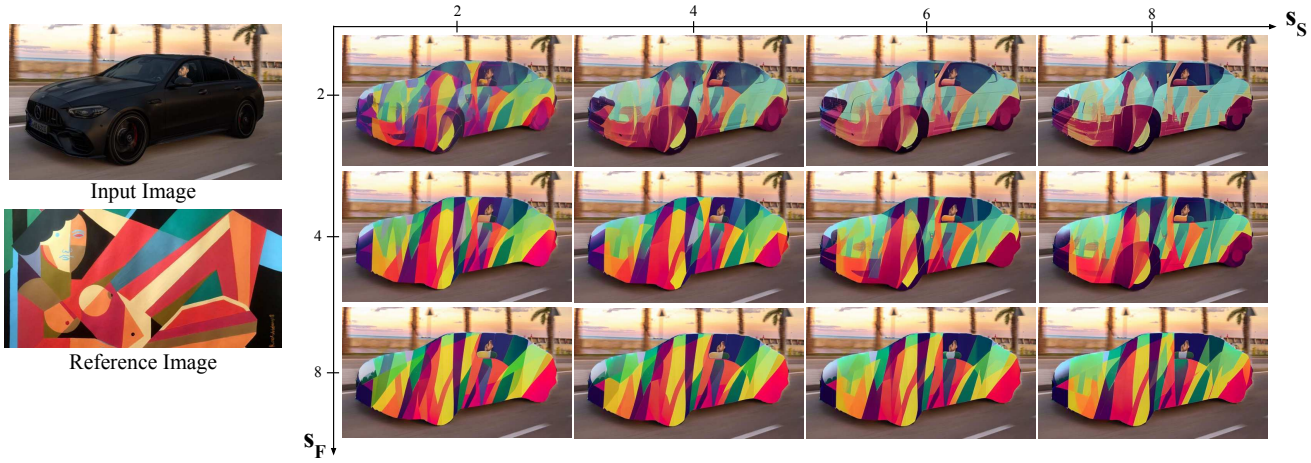

Figure 7. The figure shows the affect of s_F and s_S parameter in multimodal classifier free guidance Eq. 4 when they are varied. We can see that as we increase s_F the output forcefully imposes the appearance from the reference image and the car starts losing the structure details that were helping to make it look like a car. In order to maintain the structural integrity of the car we need to increase s_S.

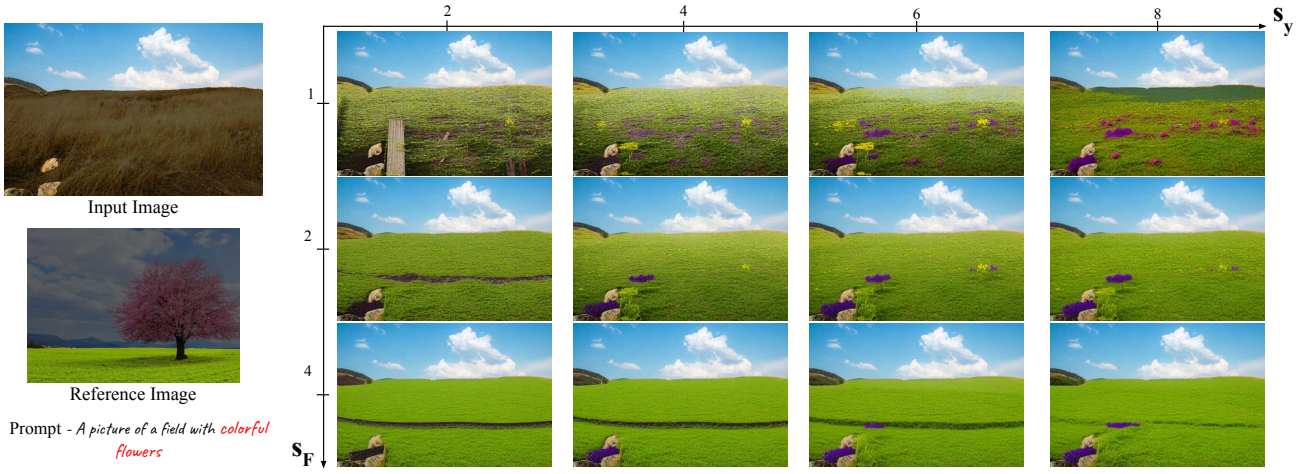

Figure 8. The figure shows the effect of s_F and s_T parameter in multimodal classifier free guidance Eq. 4 when they are varied. s_F controls the effect of the reference image and s_y control the effect of the prompt. We can see that the output is highly sensitive to s_F. Even if we increase s_F slightly the effect of the prompt starts disappearing. When we want to use both reference images and prompts to affect the final image it is best to keep $s_y > s_F$ and s_F should have a low value in an absolute sense.

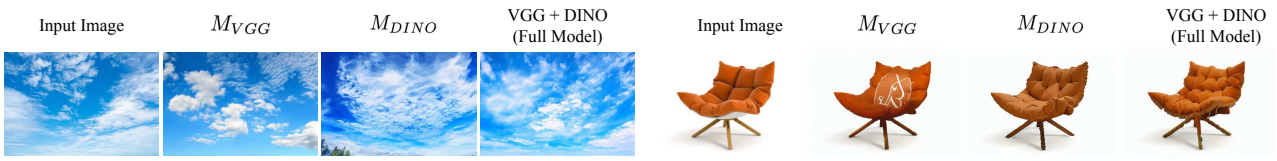

Figure 9. Object level appearance variations are shown for models trained with different appearance representations. It can be observed that M_{DINO} faces difficulty in preserving the color when generating variations. The sky is a bit darker than the input image whereas, in the case of the couch, the shade of orange color does not match the input image. We can see that M_{VGG} is able to preserve the color however it can have artifacts even for slightly complex objects. In the case of the couch, we can see some white artifacts that might have come from the white bottom of the couch in the input image. M_{VGG} have a poor understanding of objects compared to M_{DINO}. Only the full model which uses both captures the visual aspects of the object faithfully.

Base Model	Dataset	LR	Batch Size	Iterations	GPU Days
LDM	Bedroom	9.6e-5	48	750k	24
LDM	Churches	1.0e-5	96	350k	12
LDM	CelebA-HQ	9.6e-5	24	120k	1
SD + ControlNet	COCO	1.5e-5	128	86k	96

Table 4. Hyperparameters for PAIR diffusion when used with LDM [38] and Stable Diffusion (SD) with ControlNet [59].

and choose the bed as the object to edit. For each image, we randomly select a patch within the bed, and use a patch extracted in the same way from another image as the driver for the edit. Next, we describe the baselines. **Copy-Paste**: the target patch is copied and pasted in the target region of the input image, resizing the patch to fit the target region. **Inpainting**, we use the model pretrained on LSUN Bedroom Dataset by [38], and use it to inpaint the edit region. To do that, we use a masked sampling technique, as done in the inpainting task in Rombach et al. [38]. **CP+Denoise**, we start from the results of copy-paste and apply DDIM Inversion to map the image to the diffusion noise space [45]. Subsequently, we apply LDM to denoise the image to the final result. Lastly, we compare our method with **E2EVE** [3]. We use the original pre-trained weights shared by the authors and use their model to perform the edit. Next, we detail the metrics calculation pipeline. We compute *naturalness* by measuring the FID between the edited images and the original images from the whole dataset. We estimate the *locality*, by measuring the L1 loss between the original image and the edited image outside the edited region (*i.e*. the region that should not change). Finally, the *faithfulness* is measured by the SSIM between the driver image and the edited region in the edited image.

Qualitative Experiments. We run Prompt-Free-Diffusion [53] following the description in Sec. 4.5 of the paper. For implementation, we follow the author's instructions at the following GitHub issue. Specifically, we crop the input image around the object being edited and the reference image around the selected object. We feed the two crops to the SeeCoder and use the segmentation ControlNet with the segmentation map of the cropped input image as the conditioning signal. We then get the edited image by cutting the region of interest in the output image and pasting it in the input image. Regarding Paint-By-Example [54], we crop the reference image around the selected object and follow the original inference procedure afterward.

8. Qualitative Results

8.1. Stable Diffusion Results

In this section, we show additional results for PAIR Diffusion when coupled with a foundational diffusion model like Stable Diffusion [38]. In Fig. 11, we perform appearance manipulation in the wild, showing realistic edits in different scenarios. In Fig. 12, we provide additional results for the task of adding a new object to a given scene. Lastly, we showcase another capability of our model, *i.e*. producing variations of a given object. Specifically, we sample different initial latent codes $z_i \sim \mathcal{N}(0, 1)$, while fixing the structure and appearance representation. We report the results in Fig. 13.

8.2. Unconditional PAIR Diffusion

We start by providing additional results for the task of appearance control. In Fig. 10 (a), we can notice that our method can easily transfer the appearance of a church from a completely different structure in the reference image to the structure of the church in the input image. At the same time, we can copy relatively homogeneous regions like the sky, transferring the color accurately, as well as more textured objects such as the trees. In Fig. 10 (b), it is interesting to note that, when we change the style of the floor, the model can appropriately place the reflections hence realistically harmonizing the edit with the rest of the scene. Similar observations can be made when we edit the wall. Lastly, in Fig. 10 (c) we show results on faces. We can observe that our method accurately transfers the appearance from the reference image, modifying the skin, hair, and eyebrows of the input. We notice that all our edits do not alter the identity of the person in the input image, which is a desirable property when editing faces.

Next, we provide an additional qualitative comparison for the task of appearance control with the baselines detailed in Sec. 7. In Fig. 14, we can observe that our method seamlessly transfers the appearance from the reference image to the input image, while maintaining the edit to the targeted region. Moreover, we show the qualitative comparison with SEAN [62] in Fig. 15. We can see that our method gives better editing results and we also allow to control the strength of the edit. In Fig. 16, we showcase more nuanced appearance editing results instead of simply swapping the appearance of input and reference images (*i.e*. $f_i' = f_i^R$) by linearly combining the two. We exploit the flexibility of our formulation by setting $a_0 = \lambda, a_1 = 1 - \lambda$, with $\lambda \in [0, 1]$, *i.e*. interpolating input and reference images. We can notice how the appearance of the edited region smoothly transitions from the original appearance to the reference, providing an

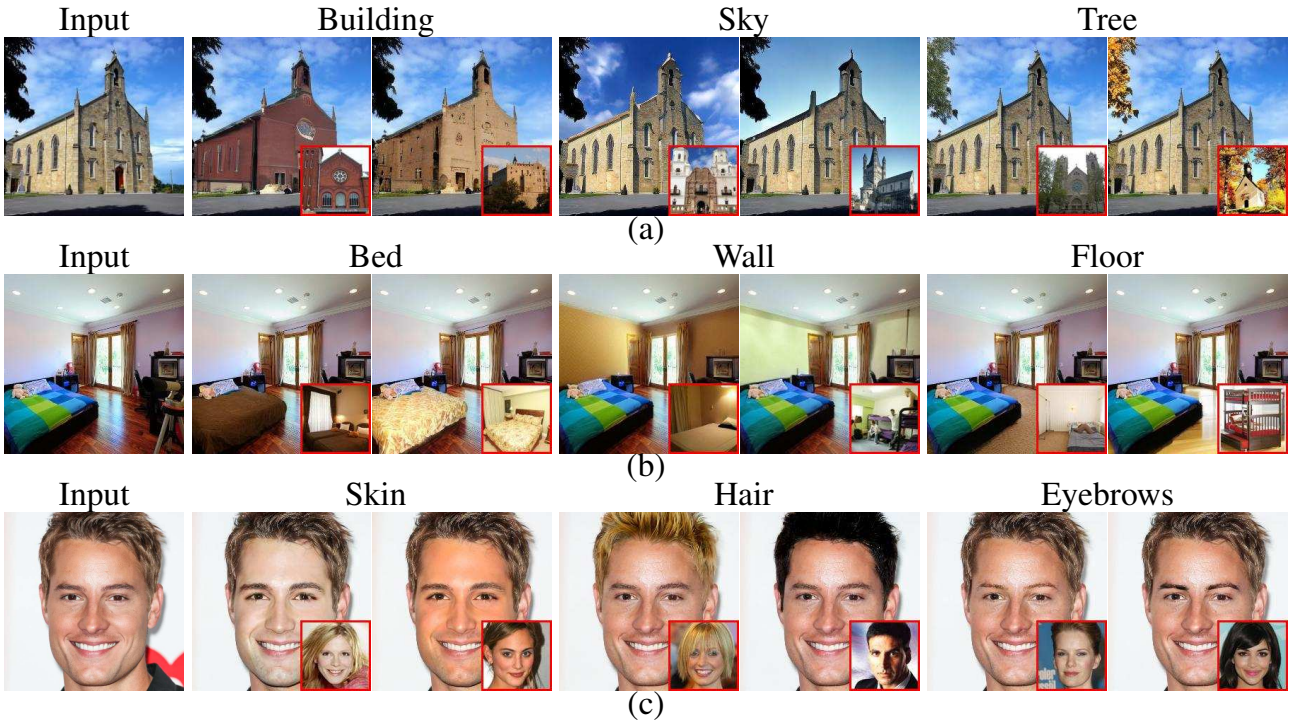

Figure 10. Qualitative results of Appearance Manipulation using UC-PAIR diffusion model. Reference images are shown in the bottom right, while the text on top indicates the object targeted by the editing operation.

additional level of control for the end user.

Lastly, we present a more challenging editing scenario using reference images that contain no semantics (*e.g.* abstract paintings) and use it to perform both localized and global editing in Fig. 17.

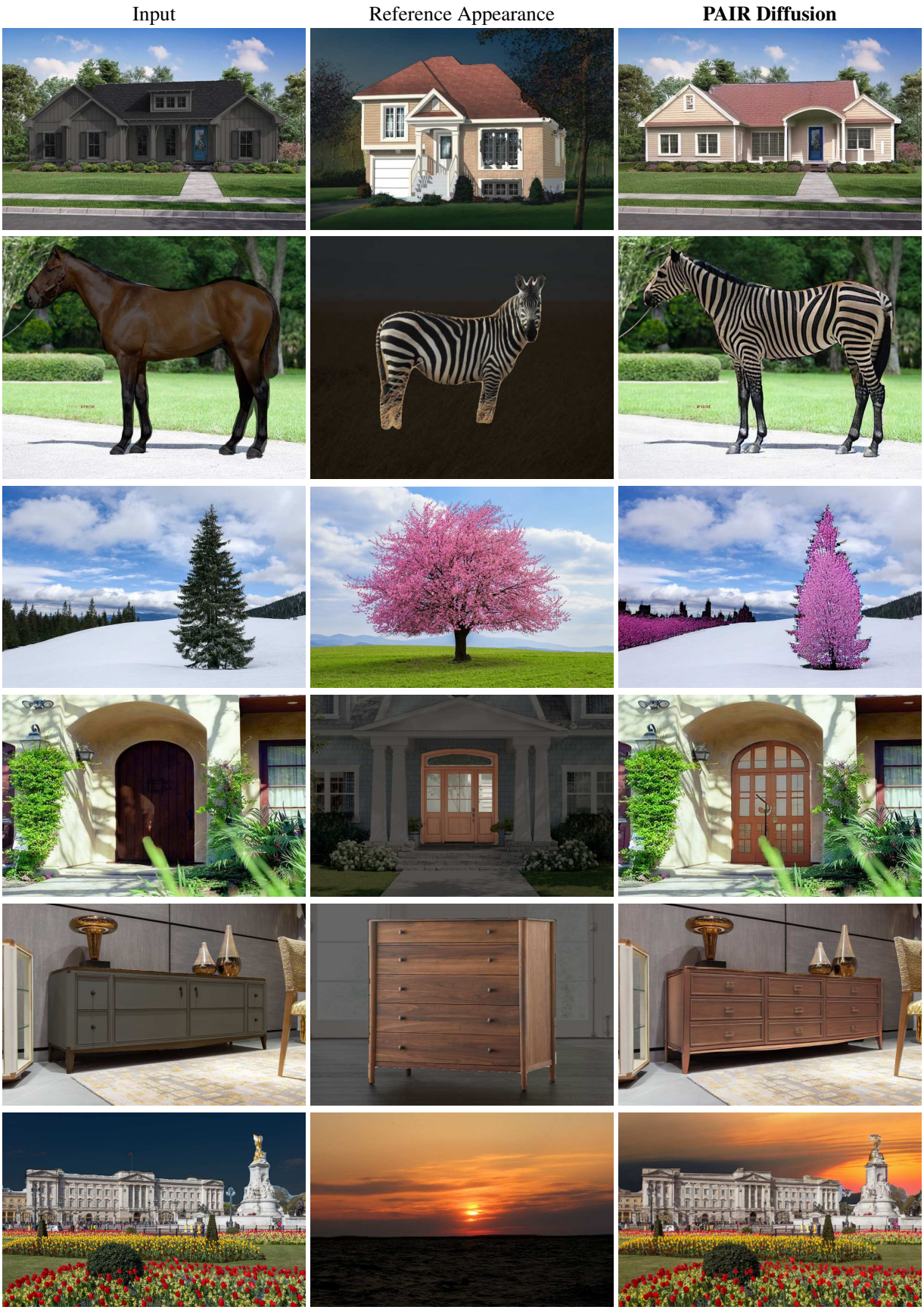

Figure 11. Appearance editing in the wild.

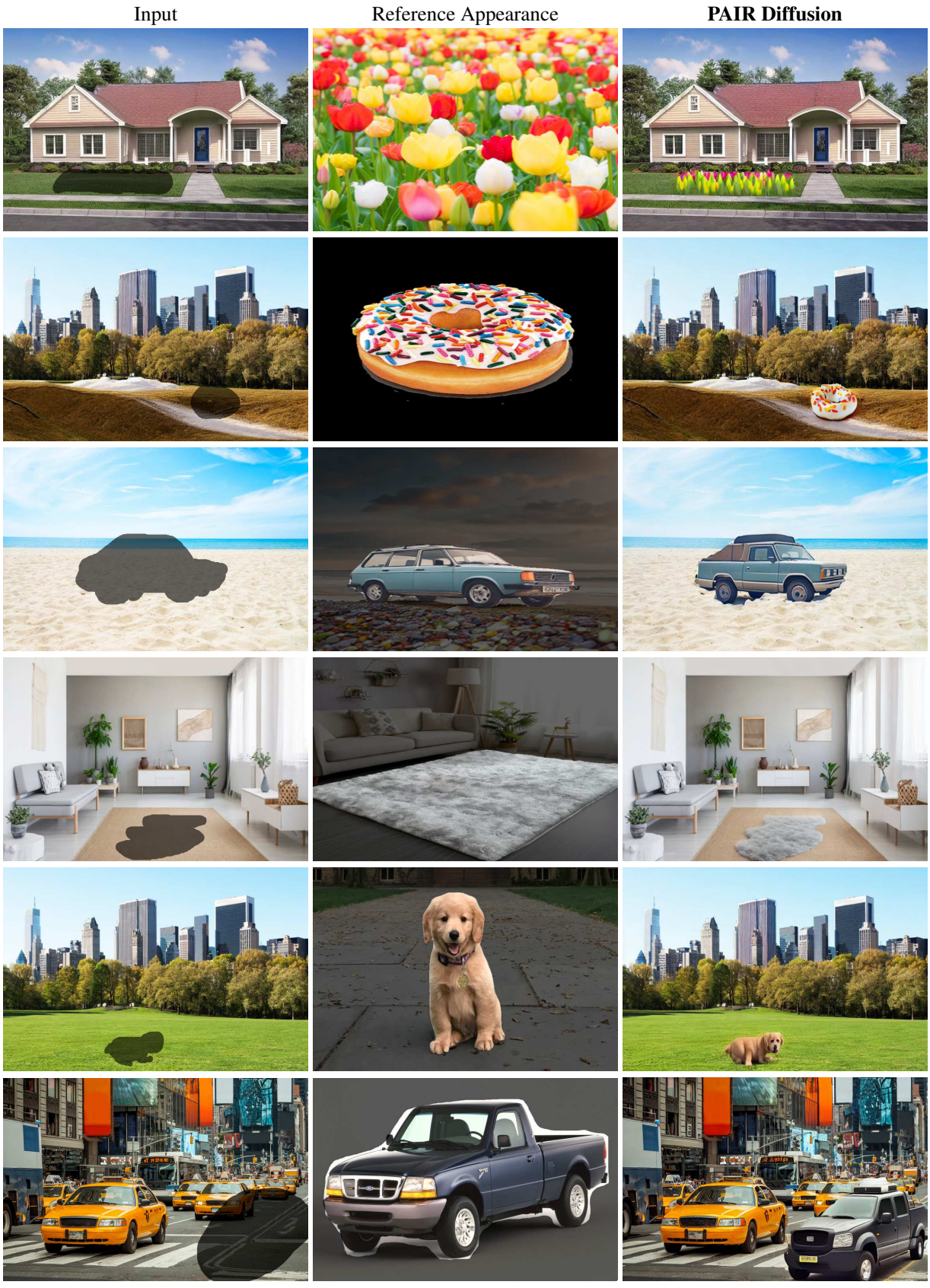

Figure 12. Add objects to the scene.

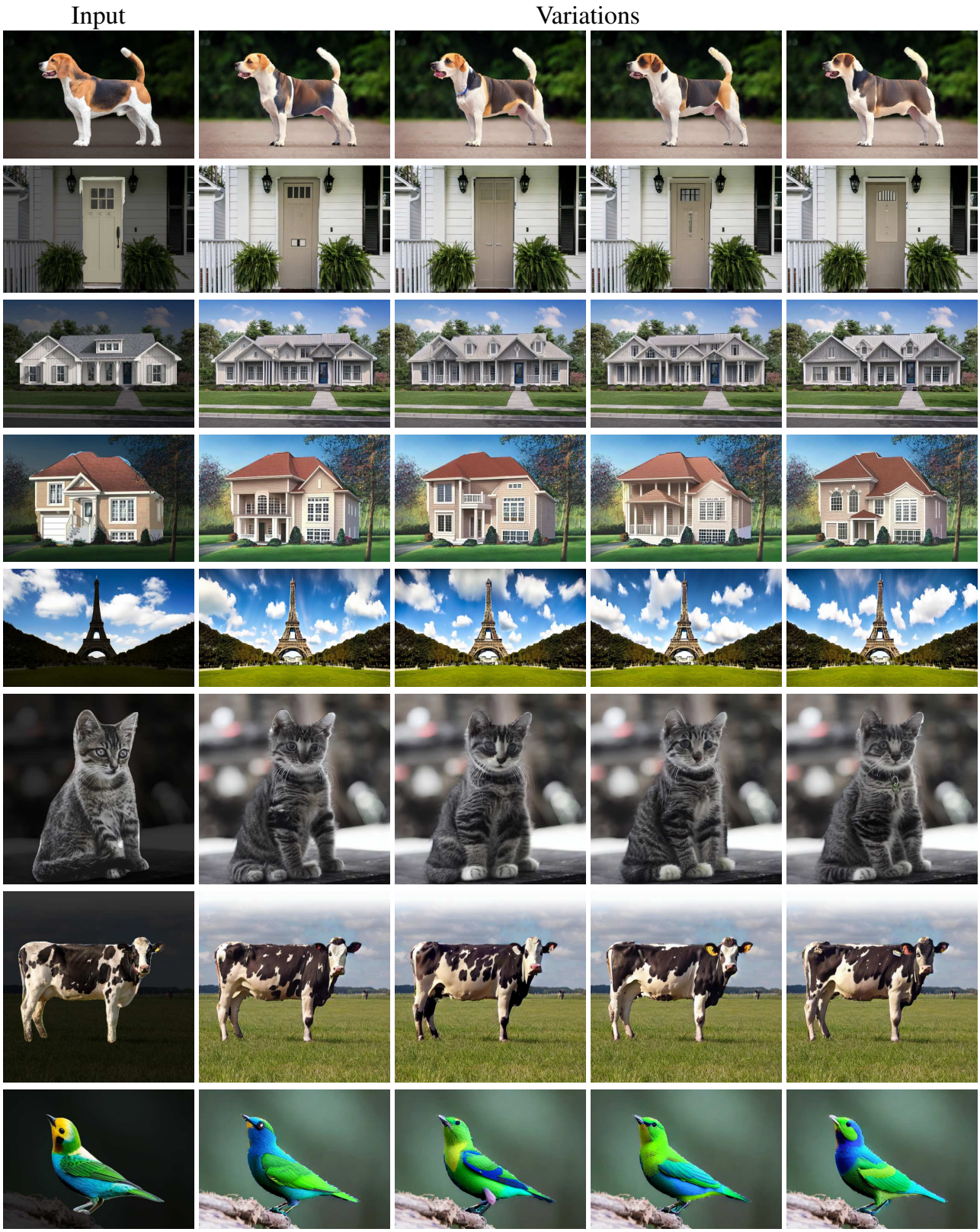

Figure 13. Object variations. We obtain variations in the appearance of the objects when generating images with different seed. This can be attributed to the lossy procedure used to obtain appearance vectors.

Figure 14. Visual results for in-domain localized image editing. We edit the input image, using as a driver the reference image, targeting the red-boxed area. With PAIR Diffusion we can perform realistic edits in challenging scenarios. For example, in the first row, we can use the entire bed as a driver and edit only a patch of the input image. On the contrary, in the last row, we use a small patch as a driver and target the whole bed of the input image for the edit. In both cases, our method outputs realistic edited images. Moreover, due to the masked DDIM technique, we introduce almost no distortion in the area outside the red box (*i.e.* the one that should not change). We show results for all the baselines. Note that unlike other results in the paper which uses edit regions specified by the user or generated using a segmentation model, here we define edit regions using predefined boxes.

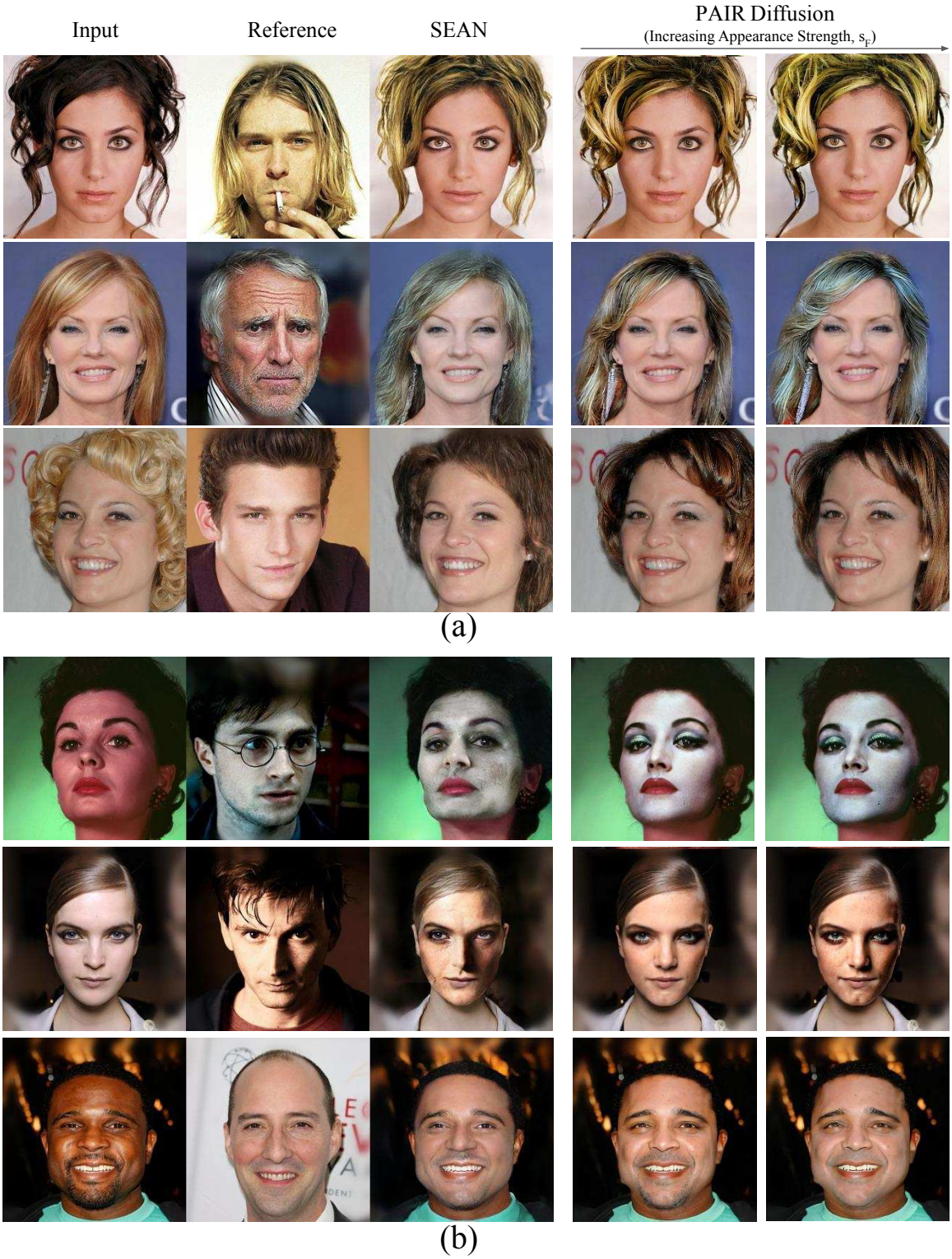

Figure 15. Qualitative comparison against SEAN [62] for editing the appearance of (a) Hair (b) Skin. Unlike SEAN [62] we can also control the edit strength using our proposed classifier free guidance Eq. (4)

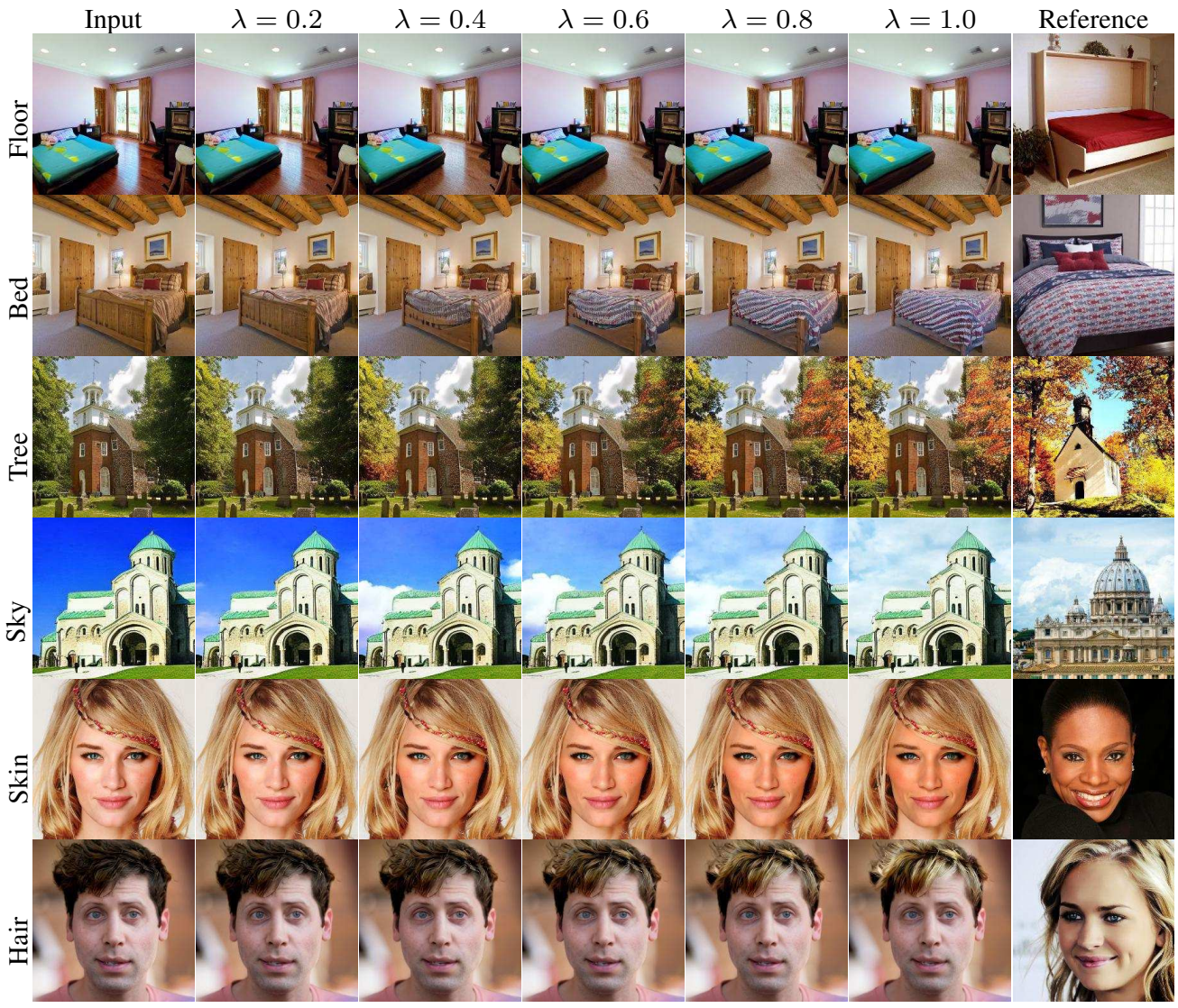

Figure 16. We can control the strength of appearance and interpolate between the reference and input appearances. We set appearance as $f' = (1 - \lambda)f_i + \lambda f_j^R$ where f_i is the input appearance and f_j^R is the reference appearance and vary λ from 0 to 1.

Figure 17. Visual results for (a) local image editing, (b) global image appearance manipulation.